

PACS numbers: 42.55.Rz; 42.70.Hj; 63.20.kd
DOI: 10.1070/QE2015v045n12ABEH015816

On the influence of the local vibration on spectral and laser characteristics of F_2^- colour centres in LiF crystals at low temperatures

A.G. Papashvili, S.N. Smetanin, M.E. Doroshenko

Abstract. **A study of spectral and laser properties of the LiF : F_2^- crystal at low temperatures has revealed an electronic–vibrational interaction of electrons of the F_2^- centre with the local vibration of the centre, which occurs against the background of coupling between electrons of F_2^- centres and lattice phonons. The interaction of electrons with the local vibration manifests itself in spectra in the form of narrow lines superimposed on wide electron–phonon lines that are due to the electron–lattice interaction. An anomalous behaviour of spectral LiF : F_2^- laser lines is also found at liquid nitrogen temperature upon selective excitation; this behaviour is explained by the difference in the probabilities of the lattice and local interactions.**

Keywords: *F_2^- colour centre, electronic–vibrational interaction, local vibration.*

1. Introduction

Lasers based on LiF : F_2^- crystals are efficient and reliable solid-state sources of tunable near-IR radiation (λ = 1.08–1.29 μm), which operate at room temperature in both nanosecond and picosecond regimes [1–7]. Since the absorption and luminescence spectra of F_2^- colour centres in LiF crystals at room temperature have a form of wide bands [8], tunable lasing can be implemented on them. The convenient spectral position of the wide (0.8–1.1 μm) absorption band makes it possible to carry out pumping using both widespread ytterbium and neodymium lasers (λ = 1.03–1.08 μm) and commercially available multimode laser diodes (λ = 0.94–0.98 μm) to implement lasing with high efficiency (up to 45%) [3–5]. LiF : F_2^- crystals were used as laser amplifiers of picosecond pulses of a $KGd(WO_4)_2 : Nd^{3+}$ laser with stimulated Raman scattering (SRS) frequency self-conversion for individual laser pulses with energies up to 30 mJ and output power as high as 10^{10} W [6, 7] and as antireflection filters for passive Q-switching of high-efficiency neodymium lasers (λ = 1.03–1.08 μm) [9–11], operating in repetitively pulsed or quasi-cw regimes. LiF : F_2^- crystals were used in [12] for passive Q-switching of the $SrMoO_4 : Nd^{3+}$ laser with SRS frequency self-conversion and for laser amplification of subnanosecond SRS pulses of the same laser. The laser properties of F_2^- colour centres in a new nanostructured LiF ceramics were investigated in [13]; it was shown that they do not differ from those in LiF crystals at room temperature. However, the spectral properties of F_2^-centres in ceramics at low temperatures have not been studied.

Despite the large number of studies devoted to application of LiF : F_2^- crystals as active elements, the mechanisms of the electronic–vibrational interaction in the colour centres of LiF crystals is still unclear. Fitchen [14] applied the single-frequency model in the Frank–Condon approximation, i.e., described only the interaction between electrons of colour centres and single-frequency lattice vibrations (electron–phonon interaction). As was shown in [15], this model describes well the spectral properties of F_2^- colour centres in LiF crystals at temperatures above 150 K. However, cooling below 150 K gives rise to a fine structure of individual spectral lines of F_2^- colour centres in LiF crystals, which cannot be described within the single-frequency model. The Debye temperature was found in [14] within this approximation based on experimental absorption spectra recorded at low temperatures; it turned out to differ significantly from the known Debye temperature values, obtained by measuring the specific heat of the LiF crystal [16]. This discrepancy is another evidence of inaccurate description of F_2^- colour centres in LiF crystals within the single-frequency model. Nahum [17] proposed to describe the structure of absorption and luminescence spectra of LiF crystals with colour centres at low temperatures (10–77 K) as a superposition of the spectra of several similar colour centres, related to the presence of impurities in crystals. It was shown in [18] that the presence of OH groups in LiF crystals facilitates the formation of F_2^--like centres with an absorption and luminescence spectral range overlapping with the absorption and luminescence range of F_2^- centres; however, a specific structure of low-temperature spectra of F_2^- colour centres in LiF crystals was observed both in the presence and in the absence of impurities.

In this paper, we report the results of studying the spectral and laser characteristics of the LiF : F_2^- crystal at low temperatures (T = 10–77 K). The spectral properties of F_2^- centres in LiF crystals are interpreted within the lattice vibration model, which includes not only vibrations of an ideal lattice but also local-mode vibrations (the latter are due to the presence of lattice vacancies). The formation of F_2^- centres is inevitably related to the generation of two neighbouring vacancies and change in the ion–ion interaction parameters for the ions surrounding a vacancy. Correspondingly, the parameters of the electronic–vibrational interaction with participation of local and lattice vibrations may differ significantly, and the vibration amplitude for the ions around a vacancy should deviate significantly from the vibration amplitudes of ideal-lattice ions at certain frequencies.

A.G. Papashvili, S.N. Smetanin, M.E. Doroshenko A.M. Prokhorov General Physics Institute, Russian Academy of Sciences, ul. Vavilova 38, 119991 Moscow, Russia; e-mail: ssmetanin@bk.ru

Received 24 March 2015; revision received 2 July 2015
Kvantovaya Elektronika **45** (12) 1111–1116 (2015)
Translated by Yu.P. Sin'kov

2. Technique and results of measuring spectral parameters

The transmission spectra of the samples at 10 K were measured using a double DFS-12 monochromator. The sample was placed in an RDK 10-320 helium cryostat (Refregerant Helium GmbH). The broadband beam transmitted through the sample was focused onto the input slit of the monochromator. A halogen lamp with a chopper (600 Hz) served as a modulated-radiation source. The radiation from the monochromator output was recorded with a FEU 83 photoelectron multiplier. The electric signal from the multiplier was applied to a Tektronix TDS 380 digital oscilloscope. The oscilloscope was triggered synchronously with the incident optical signal using a photodiode. Further processing of the oscilloscope signal was performed on a personal computer.

The transmission (absorption) spectrum of the $LiF:F_2^-$ crystal at $T = 77$ K was recorded with a two-channel SF 20 spectrophotometer. The sample was placed on a copper cold finger of the nitrogen cryostat. The sample temperature was controlled using a copper–constantan thermocouple.

The luminescence spectrum of the $LiF:F_2^-$ crystal was measured according to the scheme presented in Fig. 1 (in the absence of mirrors of the $LiF:F_2^-$ laser cavity).

The excitation source was a tunable $LiF:F_2 \rightarrow F_2^+$ laser longitudinally pumped by the second harmonic of a nanosecond Nd laser. To increase the tunable-beam selectivity, we improved the scheme of the well-known 'Malsan' $LiF:F_2 \rightarrow F_2^+$ laser [1]. The point is that, when tuning frequency in this laser, we observed, along with a narrow ($\Delta\nu = 10$ cm^{-1}) laser line, coaxial double-pass amplified spontaneous radiation on luminescence-line wings; the intensity of this radiation was comparable with the laser beam intensity.

In the improved scheme of the $LiF:F_2 \rightarrow F_2^+$ pump laser (Fig. 1), spontaneous radiation can be amplified only during one passage through the active element, due to which its influence is significantly reduced. As a result, the pump spectrum contains only a narrow laser line even when working on the luminescence line wings of the $LiF:F_2 \rightarrow F_2^+$ crystal. Figure 2 shows the tuning curve of the $LiF:F_2 \rightarrow F_2^+$ pump laser (850–1050 nm), which is in good agreement with the absorption spectrum of the $LiF:F_2^-$ crystal. The linewidth of the tunable $LiF:F_2 \rightarrow F_2^+$ laser did not exceed 1 nm.

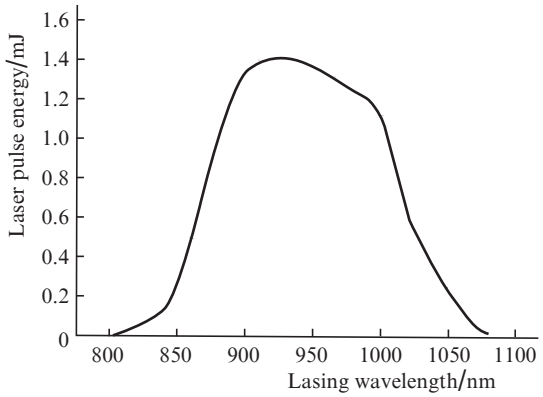

Figure 2. Tuning curve for the $LiF:F_2^-$ pump laser wavelength.

Figure 3 shows the absorption and luminescence spectra of the $LiF:F_2^-$ crystal measured at a temperature of 77 K, and Fig. 4 presents the absorption spectrum of the $LiF:F_2^-$ crystal recorded at 10 K.

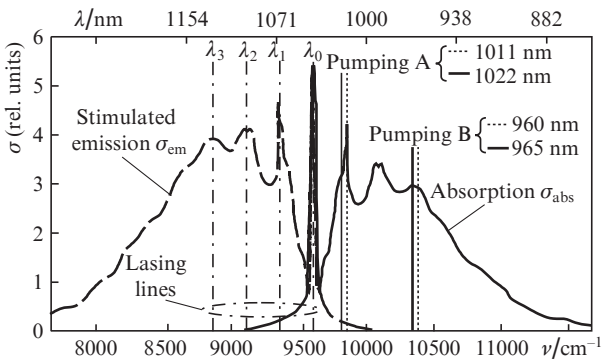

Figure 3. Absorption (solid line) and luminescence (dashed line) spectra of the $LiF:F_2^-$ crystal at 77 K. The vertical solid and dotted lines indicate the pump wavelengths (pumpings A and B) in the laser experiments upon selective excitation, and the dot-dashed lines indicate the positions of lasing lines.

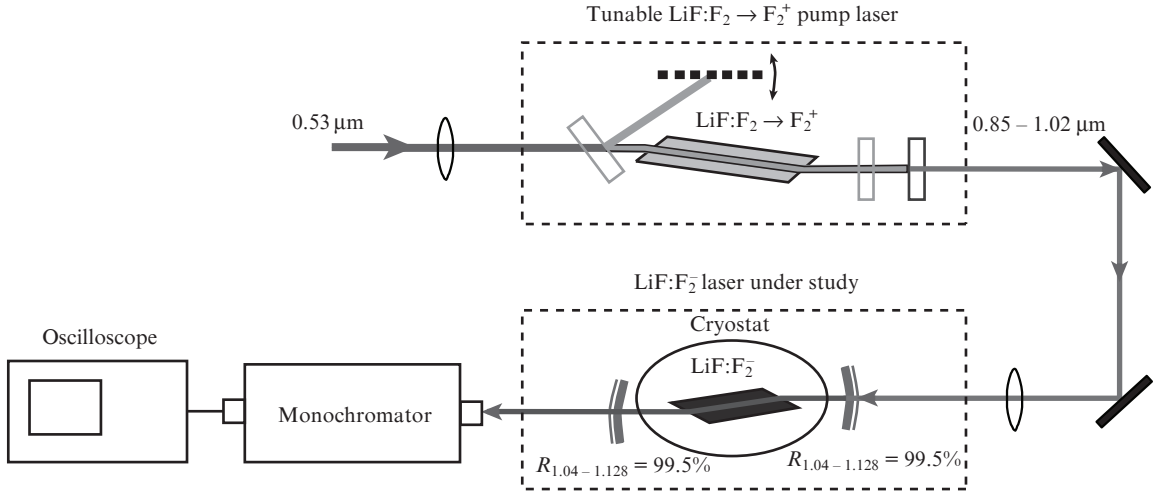

Figure 1. Schematic diagram of the experimental laser setup.

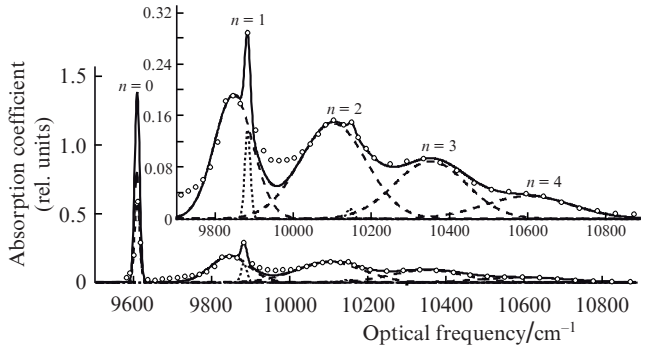

Figure 4. Absorption spectra of the LiF : F_2^- crystal at 10 K. Circles are direct measurement data. Lines are the results of processing the measurement data: dashed Gaussians describe the electronic–vibrational interactions of electrons of the F_2^- centre with the lattice, dotted Gaussians describe the interaction of electrons with the local vibration of the F_2^- centre, and the solid line is the total absorption spectrum.

3. Discussion of spectral measurement results

The absorption spectrum recorded at 10 K (see Fig. 4) contains two pronounced groups of lines. Each line can be described well by the Gaussian function

$$f_n^{\mathrm{lat,loc}}(\nu) = I_n^{\mathrm{lat,loc}} \exp\left[-\left(\frac{\nu - \nu_n^{\mathrm{lat,loc}}}{\Delta\nu_n^{\mathrm{lat,loc}}}\right)^2\right], \tag{1}$$

where n is the number of the vibrational excitation level (n = 0, 1, 2, …); $I_n^{\mathrm{lat,loc}}$ is the intensity of the nth line; $\nu_n^{\mathrm{lat,loc}}$ is its centre frequency; and $\Delta\nu_n^{\mathrm{lat,loc}}$ is its half-width at the 1/e level. The lines are located equidistantly in each group. The first-group lines (denoted by a superscript 'lat') have a large width (dashed line) and are shifted with respect to each other by $\nu_{n+1}^{\mathrm{lat}} - \nu_n^{\mathrm{lat}} = 250$ cm^{-1}. The second-group lines (denoted by a superscript 'loc') are narrow (dotted line); they are shifted by $\nu_{n+1}^{\mathrm{loc}} - \nu_n^{\mathrm{loc}} = 270$ cm^{-1}.

The phonon spectrum of the LiF crystal was reported in [19]. The energies of two acoustic phonons (0.026 eV or 210 cm^{-1} and 0.031 eV or 250 cm^{-1}) and one optical phonon (0.036 eV or 290 cm^{-1}), involved in the optical transitions of the F_2^- colour centre in the LiF crystal, were found in [20]. We can suggest that the spectrum recorded by us (see Fig. 4), which consists of wide repeating lines (dashed lines), is due to the electronic–vibrational interaction between the electrons of the F_2^- centre and the LiF crystal lattice at a phonon frequency of 250 cm^{-1} (the superscript 'lat' stands for 'lattice').

The narrow lines (dotted Gaussians) that are also observed in the spectrum in Fig. 4 were attributed in [17] to colour centres of another type; however, the results of our spectral-kinetic study of LiF : F_2^- crystals with different impurities [15] suggest that these lines are due to the local vibration of the F_2^- centre [21] (the superscript 'loc' stands for 'local') rather than to impurity centres.

Thus, the electronic–vibrational interactions of electrons with the lattice (dashed lines) and with the local vibration of the F_2^- centre (dotted line) contribute to the absorption spectrum (circles).

The parameters of all Gaussians in (1) were chosen so as to make the total spectrum (solid line) fit in the best way the experimental results.

The interactions of electrons with lattice vibrations and with the local centre vibration make different contributions to the zero-phonon line [16]; these contributions cannot be measured directly. One can see that the lines that are due to local and lattice vibrations are overlapped in the absorption spectrum. Let us artificially divide the colour centres into two groups: those involved in the local vibration only and those participating in lattice vibrations only; correspondingly, we consider the zero-phonon line as the sum of zero-phonon lines of these centres.

To determine the unknown parameters of these interactions (especially the zero-phonon line parameters), we will use the single-frequency model in the Frank–Condon approximation at a temperature close to absolute zero. The probability of the electron–phonon transition upon interaction of F_2^- centre electrons with the lattice can be expressed in terms of Pekarian [22, 23]:

$$J_n^{\mathrm{lat}} \Big/ \sum_{n=0}^{\infty} J_n^{\mathrm{lat}} = \frac{S_{\mathrm{lat}}^n}{n!}\alpha_{\mathrm{lat}}, \tag{2}$$

where $J_n^{\mathrm{lat}} = I_n^{\mathrm{lat}} \Delta\nu_n^{\mathrm{lat}} \sqrt{\pi}$ is the total intensity of the nth line of the electron–phonon spectrum (n = 0 corresponds to the zero-phonon line, and $n > 0$ corresponds to the lines describing the interactions involving n phonons); $\alpha_{\mathrm{lat}} = J_0^{\mathrm{lat}} \big/ \sum_{n=0}^{\infty} J_n^{\mathrm{lat}}$ is the Debye–Waller factor, which is the normalised total intensity of the zero-phonon line for the electronic–vibrational interaction with the lattice; and $S_{\mathrm{lat}} = -\ln\alpha_{\mathrm{lat}} = J_1^{\mathrm{lat}}/J_0^{\mathrm{lat}}$ is the Huang–Rhys factor, which is the ratio of the total intensities of the one-phonon and zero-phonon lines for the same type of interaction. We assume that a similar expression can be written for the interaction with the local vibration of the F_2^- centre:

$$J_n^{\mathrm{loc}} \Big/ \sum_{n=0}^{\infty} J_n^{\mathrm{loc}} = \frac{S_{\mathrm{loc}}^n}{n!}\alpha_{\mathrm{loc}}, \tag{3}$$

where α_{loc} and $S_{\mathrm{loc}} = -\ln\alpha_{\mathrm{loc}}$ are, respectively, the Debye–Waller and Huang–Rhys factors for the interaction with the local vibration of the F_2^- centre and $J_n^{\mathrm{loc}} = I_n^{\mathrm{loc}} \Delta\nu_n^{\mathrm{loc}} \sqrt{\pi}$ is the total intensity of the nth line in the spectrum corresponding to the interaction with the local vibration of the F_2^- centre.

The ratio of the total line intensities for the transitions with participation of one and two phonons in the case of interaction with local vibration will be denoted as parameter γ:

$$\gamma = \frac{J_2^{\mathrm{loc}}}{J_1^{\mathrm{loc}}}. \tag{4}$$

Having replaced the total intensities $J_{1,2}^{\mathrm{loc}}$ in (4) according to formula (3), we find that

$$S_{\mathrm{loc}} = 2\gamma. \tag{5}$$

According to the data of Fig. 4 (dashed Gaussians), $\gamma = 0.13$; then, $S_{\mathrm{loc}} = 0.26$ and $\alpha_{\mathrm{loc}} = 0.77$.

Let us now find the Debye–Waller and Huang–Rhys factors (α_{lat} and S_{lat}, respectively) for the interaction with the lattice.

The total intensities of the wide lines of the phonon wing (dashed Gaussians in Fig. 4), normalised to the area of the entire phonon wing (with the zero-phonon line excluded), can be measured exactly. Their experimental values are given by the formula

$$P_n^{\mathrm{exp}} = J_n^{\mathrm{lat}} \Big/ \sum_{n=1}^{\infty} J_n^{\mathrm{lat}}. \tag{6}$$

At the same time, they can be found theoretically according to formula (2):

$$P_n^{\text{theor}} = \frac{\alpha_{\text{lat}}}{1-\alpha_{\text{lat}}}\frac{(-\ln\alpha_{\text{lat}})^n}{n!}, \quad (7)$$

where α_{lat} is the desired parameter. Having analysed (using the least-squares method) the convergence of the values given by expressions (6) and (7),

$$\frac{\mathrm{d}}{\mathrm{d}\alpha_{\text{lat}}}\sum_{n=1}^{\infty}(P_n^{\text{theor}} - P_n^{\text{exp}})^2 = 0, \quad (8)$$

we obtain the sought-for value $\alpha_{\text{lat}} = 0.13$ (and $S_{\text{lat}} = -\ln\alpha_{\text{lat}} = 2.04$), which corresponds to the least rms deviation of theoretical values P_n^{theor} from experimental values P_n^{exp}. As a result, we have $P_1^{\text{theor}} = 0.305$ and $P_1^{\text{exp}} = 0.277$, $P_2^{\text{theor}} = 0.311$ and $P_2^{\text{exp}} = 0.368$, $P_3^{\text{theor}} = 0.211$ and $P_3^{\text{exp}} = 0.239$, and $P_4^{\text{theor}} = 0.108$ and $P_4^{\text{exp}} = 0.058$.

As in the spectra measured at a temperature of 10 K, the absorption and luminescence spectra recorded at 77 K (Fig. 3) contain a narrow ($\Delta\nu \approx 10$ cm^{-1}) zero-phonon line, peaking at a wavelength of 1.0404 μm, and wide lines due to electron–phonon transitions, spaced by frequency intervals of about 250 cm^{-1}; these lines are mirror-symmetric with respect to the zero-phonon line.

Both the absorption and luminescence spectra (Fig. 3) contain a narrow peak, which is due to the interaction of electrons of F_2^- centre with the local vibration of this centre. This peak lies on the wing of the first wide electron–phonon line and is shifted with respect to the zero-phonon line by 270 cm^{-1}. The peak of the second electron–phonon line has a fine structure, which can also be explained [by analogy with the absorption spectrum measured at 10 K (Fig. 4)] by the presence of a weak (second) narrow peak, related to the interaction of the electron with the local vibration. The ratio of the intensities of the second and first narrow peaks, according to formulas (4) and (5), yields approximately the same value of the Huang–Rhys factor for the interaction with the local vibration as at 10 K ($S_{\text{loc}} \approx 0.26$). Processing of the 77-K data (Fig. 3) according to formulas (6)–(8) yielded $\alpha_{\text{lat}} = 0.068$ and $S_{\text{lat}} = -\ln\alpha_{\text{lat}} = 2.69$.

Thus, an increase in temperature from 10 to 77 K leads to a decrease in the normalised total intensity of the zero-phonon line (the Debye–Waller factor), which is due to the electronic–vibrational interaction with the LiF:F_2^- lattice, by a factor of about two (from $\alpha_{\text{lat}} = 0.13$ to $\alpha_{\text{lat}} = 0.068$), whereas the intensity of the line due to the interaction with local vibration barely changes [$\alpha_{\text{loc}} = \exp(-S_{\text{loc}}) \approx 0.77$].

4. Lasing spectra under selective pumping of the LiF:F_2^- crystal

Figure 5 shows the LiF:F_2^--laser spectra measured at a temperature of 77 K under selective pumping by a tunable LiF:$F_2 \rightarrow F_2^+$ laser into the first (pumping A) and third (pumping B) absorption lines (see Fig. 3) of the LiF:F_2^- crystal.

Figure 6 presents a decomposition of the lasing spectrum (Fig. 5b, pumping with λ = 960 nm) into the components determined by the contributions from the interaction of electrons with different vibrations of the LiF:F_2^- lattice. It can be seen that the lasing peak at $\lambda_1 \approx 1070$ nm corresponds to the one-phonon transition with a frequency of 270 cm^{-1} (local vibration of the F_2^- centre). One can also see that the lasing line at $\lambda_2 \approx 1100$ nm is due to the two-phonon transitions for both the fundamental (2×250 cm^{-1}) and other (2×290 and 290 + 350 cm^{-1}) lattice vibrations; however, the peak of this lasing line corresponds to the two-phonon transition with a frequency of 2×270 cm^{-1}, which is due to the local vibration of the F_2^- centre.

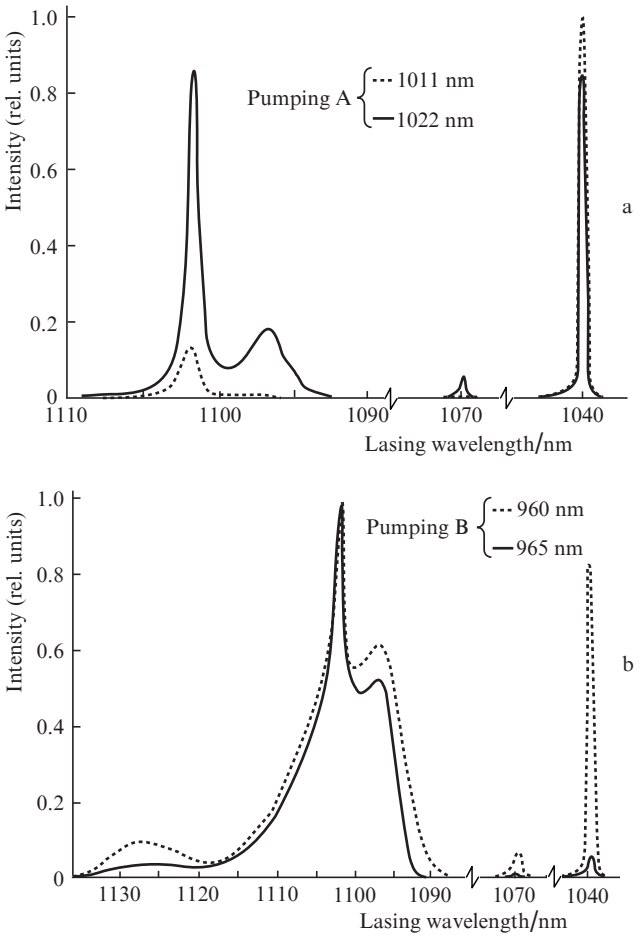

Figure 5. Lasing spectra of the LiF:F_2^- crystal at 77 K under selective pumping into (a) the first (pumping A) and (b) the third (pumping B) absorption peaks (see Fig. 3). The spectra obtained by pumping with wavelengths of 1011 and 960 nm and with wavelengths of 1022 and 965 nm are shown by dotted and solid lines, respectively.

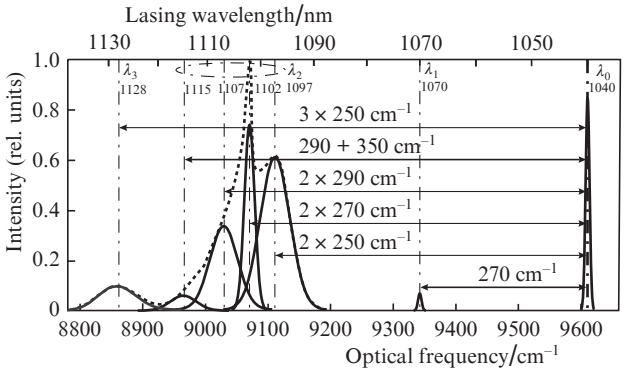

Figure 6. Decomposition of a lasing spectrum (Fig. 5b, pumping at 960 nm) into the components determined by the interactions of electrons with different vibrations of the LiF:F_2^- lattice.

Note that the beam intensity of the tunable $LiF:F_2 \rightarrow F_2^+$ laser used for pumping is close to a maximum in the wavelength range of 960–965 nm (pumping B), whereas a conversion of the radiation wavelength to the range of 1011–1022 nm (pumping A) reduces the intensity by a factor of about 2 (Fig 2).

It follows from Fig. 5a that, under pumping exactly into the narrow peak of the first absorption line with a wavelength of 1011 nm (dotted line), the lasing was developed basically on the zero-phonon (zero) luminescence line with a wavelength λ_0 = 1040 nm and on the luminescence line with a wavelength λ_2 = 1102 nm, which is due to the two-phonon 2×270 cm^{-1} transition (Fig. 6). Lasing was practically absent on other luminescence lines, including the first line (λ_1 = 1070 nm). Based on the aforesaid, one can conclude that, upon excitation into the local-vibration peak, lasing develops mainly on the transitions due to the local vibration, including the zero-phonon transition, whereas the transitions due to the interaction with the lattice are hardly involved in this process.

Figure 5a shows also a lasing spectrum (solid line) at a small shift of the pump line from the peak of the first absorption line (λ = 1011 nm) to λ = 1022 nm (see also Fig. 3, pumping A), which corresponds to the resonance of the one-phonon transition due to the electron–lattice interaction. The pump intensity barely changed under these conditions. However, as can be seen from Fig. 5a (solid line), the lasing intensity in the vicinity of $\lambda_2 \approx$ 1100 nm increased significantly, both at the wavelength of the transition involving the local vibration (peak at λ_2 = 1102 nm) and at the wavelength of the transition with participation of the lattice vibration (peak at λ_2 = 1097 nm). In addition, weak lasing arose at the wavelength λ_1 = 1070 nm, which corresponds to the transition involving the local vibration (see Fig. 6), whereas the lasing intensity on the zero-phonon transition (λ_0 = 1040 nm) slightly decreased.

Thus, one-phonon excitation of the electronic–vibrational interaction with the lattice caused lasing not only on 'lattice' luminescence lines but also on 'local' lines, in contrast to the excitation of the interaction with the local vibration, when lasing lines were only 'local'. This fact calls for a further study with due regard to the local vibration of the F_2^- centre.

The situation changes when passing to selective excitation of transitions to higher energy levels. Figure 5b shows the case of excitation of a three-phonon transition involving lattice (965 nm) and local (960 nm) transitions, with a pump intensity increased by a factor of about two (in comparison with the previous case). Due to an increase in the pump intensity, the excitation of the high-energy local transition (960 nm) provides a higher intensity throughout the entire lasing spectrum than in the case of excitation of the high-energy lattice transition (965 nm). A noteworthy fact is that the lasing intensity on the zero-phonon line significantly increased (Fig. 5b, dotted line). This behaviour of the zero-phonon line upon high-intensity excitation of transitions to high-energy levels also calls for an additional study, with allowance for the local vibration of the F_2^- centre. Then, it is necessary to perform a complementary study in order to find out why the lasing efficiency on the electronic–vibrational transition (at a wavelength of 1070 nm) with participation of one phonon is lower than on the electronic–vibrational transitions involving two phonons.

Figure 7 shows experimental dependences of the total intensities of individual $LiF:F_2^-$-laser lines on the pump pulse energy (pumping B, 960 nm). It can be seen that the lasing on the lines with $\lambda_0 \approx$ 1040 nm and $\lambda_1 \approx$ 1070 nm is least efficient, despite the fact that the peak stimulated emission cross sections are largest at these wavelengths (Fig. 3). This is due to the strong absorption of radiation at lasing wavelengths. The most efficient lasing is observed on the lines with wavelengths λ_2 = 1097 nm, λ_2 = 1102 nm and λ_3 = 1128 nm, which are characterised by zero absorption.

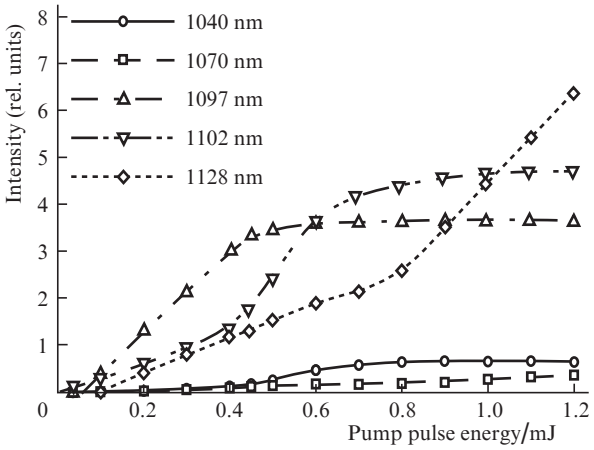

Figure 7. Experimental dependences of the total intensities of individual lasing lines of the $LiF:F_2^-$ laser on the pump pulse energy (pumping B, 960 nm).

The output radiation intensity ceases to grow with an increase in the pump energy. The reason is the excitation of a significant part of active particles under high-intensity pumping. However, the two lines with the largest wavelengths (λ_2 = 1102 nm and λ_3 = 1128 nm) exhibit anomalous behaviour: the output intensity is not saturated but starts increasing at the instant when the intensities of all other lasing lines undergo saturation. This fact can be explained by the difference in the probabilities of electronic–vibrational interactions of two types: with lattice vibrations and with local vibrations of F_2^- centres.

5. Conclusions

The study of the spectral and laser properties of the $LiF:F_2^-$ crystal at low temperatures revealed the electronic–vibrational interaction with the local vibration of the F_2^- centre, which occurs against the background of the interaction between the electrons of F_2^- centres and lattice phonons. The interaction of electrons with the local vibration manifests itself in the spectra in the form of narrow lines, imposed on the wide line that is due to the electron–phonon interaction with the crystal lattice. With an increase in temperature from 10 to 77 K, the Debye–Waller factor for the electron–lattice interaction decreases almost by half (from 0.13 to 0.068); at the same time, it barely changes (being of about 0.77) for the interaction with the local vibration. We also revealed an anomalous behaviour of the intensities of $LiF:F_2^-$ laser lines at 77 K upon selective excitation, which can be explained by the difference in the probabilities of the lattice and local interactions. Further study and mathematical simulation must be performed to reveal the contribution of the local vibration of the F_2^- centre to the lasing in the $LiF:F_2^-$ crystal at low temperatures.

Acknowledgements. We are grateful to K.K. Pukhov for the discussion of the results. This work was supported in part by the Russian Science Foundation (Grant No. 14-22-00248).

References

1. Basiev T.T., Zverev P.G., Karpushko F.V., Konyushkin V.A., Kulashik S.M., Mirov S.B., Morozov V.P., Motkin V.S., Papashvili A.G., Saskevich N.A., Sinitsyn G.V., Fedorov V.V. *Izv. Akad. Nauk SSSR, Ser. Fiz*., **54**, 1450 (1990).
2. Gellermann W. *J. Phys. Chem. Solids*, **52**, 249 (1991).
3. Basiev T.T., Zverev P.G., Mirov S.B. In: *Handbook of Laser Technology and Applications*. Ed. by C.E.Webb, J.D.C. Jones (Bristol, Phyladelphia: IOP Publishing Ltd, 2004).
4. Basiev T.T., Zverev P.G., Papashvili A.G., Fedorov V.V. *Kvantovaya Elektron.*, **24**, 591 (1997) [*Quantum Electron*., **27**, 574 (1997)].
5. Basiev T.T., Vassiliev S.V., Konjushkin V.A., Gapontsev V.P. *Opt. Lett*., **31**, 2154 (2006).
6. Basiev T.T., Garnov S.V., Vovchenko V.I., Karasik A.Ya., Klimentov S.M., Konyushkin V.A., Kravtsov S.B., Malyutin A.A., Papashvili A.G., Pivovarov P.A., Chunaev D.S. *Kvantovaya Elektron*., **36**, 609 (2006) [*Quantum Electron*., **36**, 609 (2006)].
7. Chunaev D.S., Basiev T.T., Konushkin V.A., Papashvili A.G., Karasik A.Ya. *Laser Phys. Lett*., **5**, 589 (2008).
8. Martynovich E.F., Grigorov V.A. *Fiz. Tverd. Tela*, **22**, 1543 (1980).
9. Ivanov N.A., Parfianovich I.A., Khulugurov V.M., Chepurnoi V.A. *Izv. Akad. Nauk SSSR, Ser. Fiz*., **46**, 1985 (1982).
10. Basiev T.T., Lucianetti A., Weber R., Hodel W., Weber H.P., Papashvili A.G., Konyushkin V.A. *Appl. Opt*., **38**, 1777 (1999).
11. Basiev T.T., Garnov S.V., Klimentov S.M., Pivovarov P.A., Gavrilov A.V., Smetanin S.N., Solokhin S.A., Fedin A.V. *Kvantovaya Elektron*., **37**, 956 (2007) [*Quantum Electron*., **37**, 956 (2007)].
12. Basiev T.T., Smetanin S.N., Fedin A.V., Shurygin A.S. *Kvantovaya Elektron*., **40**, 704 (2010) [*Quantum Electron*., **40**, 704 (2010)].
13. Basiev T.T., Doroshenko M.E., Konyushkin V.A., Osiko V.V., Ivanov L.I., Simakov S.V. *Kvantovaya Elektron*., **37**, 989 (2007) [*Quantum Electron*., **37**, 989 (2007)].
14. Fitchen D.B. In: *Physics of Color Centers*. Ed. by W. Beall Fowler (New York: Acad. Press Inc., 1968).
15. Basiev T.T., Dergachev A.Yu., Mirov S.B., Papashvili A.G., Orlovsky Yu.V., Osiko V.V., Konushkin V.A. *QELS Tech. Digest*, **13**, 72 (1992); Basiev T.T., Zverev P.G., Mirov S.B., Papashvili A.G., Tsintsadze G.A. *Proc. 5th Intern. Conf. 'Tunable Lasers'* (Irkutsk: Irkutsk State Univ., 1989).
16. Maradudin A. *Defects and Vibrational Spectrum of the Crystal* (New York: Wiley, 1968); Maradudin A.A. *Solid State Phys*., **19**, 1 (1966).
17. Nahum Q.J. *Phys. Rev*., **158**, 814 (1967).
18. Basiev T.T., Karasik A.Ya., Konyushkin V.A., Papashvili A.G., Pukhov K.K., Ermakov I.V., Gellerman V. *Kvantovaya Elektron.*, **32**, 659 (2002) [*Quantum Electron*., **32**, 659 (2002)].
19. Dolling G., Smith H.G., Nicklow R.M., Vijayaraghavan P.R., Wilkinson M.K. *Phys. Rev*., **168** (3), 970 (1968).
20. Farge Y., Fontana M.P. *Solid State Commun*., **10**, 333 (1972).
21. Osad'ko I.S. *Usp. Fiz. Nauk*, **128**, 31 (1979).
22. Pekar S.I. *Zh. Eksp. Teor. Fiz*., **20**, 510 (1950).
23. Huang K., Rhys A. *Proc. Roy. Soc. A*, **204**, 406 (1950).